Carbohydrate Polymers 282 (2022) 119060

Contents lists available at ScienceDirect

Carbohydrate Polymers

journal homepage: www.elsevier.com/locate/carbpol

One-pot treatment of cellulose using iron oxide catalysts to produce nanocellulose and water-soluble oxidised cellulose

Poornima Vijay [a], Warren Batchelor [b,*], Kei Saito [a,c,**]

[a] School of Chemistry, Monash University, Clayton, VIC 3800, Australia
[b] BioPRIA, Chemical Engineering Department, Monash University, Melbourne, VIC 3800, Australia
[c] Graduate School of Advanced Integrated Studies in Human Survivability, Kyoto University, Higashi-Ichijo-Kan, Yoshida-nakaadachicho 1, Sakyo-ku, Kyoto 606-8306, Japan

ARTICLE INFO

Keywords:
Nanocellulose fibres
Water-soluble oxidised oligomeric cellulose
Iron oxide catalysts
Cellulose fibrillation
Cellulose oxidation

ABSTRACT

This research explains the one-pot process of cellulose fibrillation to procure nanocellulose fibres and water-soluble oxidised cellulose using iron oxide catalysts with hydrogen peroxide. The process involved three stages. First, cellulose underwent depolymerisation to form nanocellulose fibres. Second, nanocellulose was oxidised to a water-soluble product, and the final stage was the complete decomposition. Factors such as the valency of ions in the crystal lattice of catalyst, its particle size, and reaction time influenced the treatment. By controlling these factors, either nanocellulose fibres or water-soluble oxidised cellulose with high yields of 83% and 38% produced, respectively. Nanocellulose had 73% crystallinity with DP (degree of polymerisation), 150, and the dimension of 30–110 nm thickness and 1–5 μm in length. The water-soluble product was oxidised with a carboxyl content of 2.9 mmol/g and DP, 25. This research gave an alternative method and eliminated the need for halogenated reagents, strong acids, and mechanical pretreatments.

1. Introduction

Nanocellulose fibres and water-soluble cellulose derivatives play significant roles in many polymeric materials, foods, cosmetics, and medical applications due to the abundant starting material, low cost, renewability, biodegradability, biocompatibility, and nontoxic nature (Collinson & Thielemans, 2010; Florence & Attwood, 2016).

Nanocellulose fibres are nano-size biopolymers largely focused because of their substantial surface-to-volume ratio, excellent strength, and high Young's modulus. Nanocellulose fibres are widely used to prepare many valuable products like nanostructured biocomposites, tough hydrogels, aerogel membranes, transparent paper, and films (Abitbol et al., 2016). Recently, nanocellulose has been utilised in many synthetic biology applications. Nanocellulose paper, when used as a substrate in fabricating lipid vesicles, drastically reduces the cost associated with the process (Pazzi & Subramaniam, 2020). Additionally, nanocellulose fibres are extensively used in grafting stimuli-responsive polymers from or onto their surface (Li et al., 2019; Wohlhauser et al., 2018).

Water-soluble carboxylated cellulose derivatives also present excellent physical properties like rheological and gel-forming, complexation, anti flocculation, adhesion, and superior gas barrier properties. They have proven several medical applications (Dimitrijevich et al., 1990).

One of the conventional methods of synthesising nanocellulose fibres is the fibrillation of purified pulp. High mechanical forces like high-pressure homogeniser, micro fluidiser or grinders are applied to obtain high crystalline, nanometre scale cellulose fibres. The high energy consuming process of fibrillation negatively affects the economy of nanocellulose production (Liu et al., 2017). One of the most utilised chemical pretreatment methods is using nitroxyl radicals such as 2,2,6,6-tetramethylpiperidine-1-oxyl (TEMPO) and *N*-hydroxyphthalimide in the presence of halogenated compounds like NaBr and $NaOCl/NaClO_2/NaIO_4$ as oxidants (Isogai et al., 2018). Synthetic preparation of water-soluble oxidised cellulose derivatives with high yield is

Abbreviations: Water-IF, water insoluble fraction; Water-SF, water soluble fraction; nm-Fe_2O_3, 50 nanometre size Fe_2O_3; μm-Fe_2O_3, 1 μm size Fe_2O_3; nm-Fe_3O_4, 50 nm size Fe_3O_4; μm-Fe_3O_4, 1 μm size Fe_3O_4; DP, degree of polymerisation; BEK cellulose, bleached eucalyptus kraft cellulose; DS, degree of substitution.

* Corresponding author.
** Corresponding author at: Graduate School of Advanced Integrated Studies in Human Survivability, Kyoto University, Higashi-Ichijo-Kan, Yoshida-nakaadachicho 1, Sakyo-ku, Kyoto 606-8306, Japan / School of Chemistry, Monash University, Clayton, VIC 3800, Australia.
E-mail addresses: warren.batchelor@monash.edu (W. Batchelor), saito.kei.1y@kyoto-u.ac.jp (K. Saito).

https://doi.org/10.1016/j.carbpol.2021.119060
Received 16 September 2021; Received in revised form 20 December 2021; Accepted 26 December 2021
Available online 5 January 2022
0144-8617/

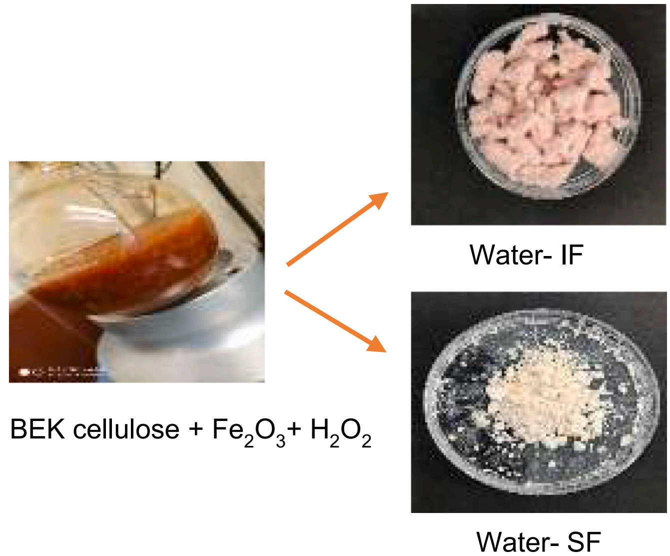

Fig. 1. Reaction mixture, Water-IF (after 1.5-hour reaction) and Water-SF (after 9-hour reaction).

possible by disordering the highly crystalline structure of the cellulose either by mercerisation or ball milling regeneration and treating the disordered cellulose with TEMPO-halogenated oxidants (Isogai et al., 2009). The main two drawbacks of TEMPO oxidation are the inability to oxidise native cellulose to water-soluble cellulose derivatives without any pretreatment methods and hazardous halogenated oxidising agents, which has a tremendous impact on the aquatic environment.

Other methods utilised to obtain cellulose nanofibres and lower molecular water-soluble cellulose derivatives are either by hydrolysis (Khan et al., 2018; Li et al., 2017) or by the action of enzymes (Elschner et al., 2018). The hydrolysis method utilises strong acids to break the glycosidic bonds in cellulose, whereas enzymatic methods are expensive and time-consuming (Coseri, 2017). Hence, this research aims to develop a single-step process by utilising very mild reagents to produce nanocellulose fibre and water-soluble cellulose derivative from native cellulose (without any pretreatment).

Iron is abundantly available, nontoxic and present in several oxidation states. Elemental iron is rarely found in nature. Iron occurs in Fe^{2+} or Fe^{3+} oxidation states, which readily combines with oxygen in nature to form its oxides. Superparamagnetic iron oxide (γ-Fe_2O_3 and Fe_3O_4) have been extensively used in biomedical applications in the past two decades (Arami et al., 2015). Iron oxide nanoparticles at lower concentrations (≤100 μg/ml) have proven to be nontoxic for biomedical applications. In terms of in vivo cytotoxicity, the highly reactive ROS (reactive oxygen species) generated by Fe^{2+} ions by reacting with the hydrogen peroxide in the mitochondria could damage the cells. As a result, magnetite (Fe_3O_4, with Fe^{2+} and Fe^{3+} ions) show higher cell toxicity as compared to that of maghemite (Fe_2O_3 with Fe^{3+} ions) (Singh et al., 2010).

Iron at concentration 0.3 mg/l in drinking water provides health benefits in humans because iron helps transport oxygen in the blood. Higher than 0.3 mg/l concentration in drinking water is involved in aesthetic issues, such as taste, odour, colour, corrosivity and staining properties (Colter & Mahler, 2006). Even though iron possesses aesthetic issues at higher concentrations in freshwater bodies, various

Table 1
Carboxyl content, DP, and DS of Water-SF and Water-IF obtained by reaction of cellulose with μm-Fe_2O_3 at different time intervals.

Entry	No of hours	Carboxyl content Water-SF (mmol/g)	DS of Water-SF	Carboxyl content of Water-IF (mmol/g)	DP of Water-SF	DP of Water-IF
1	0 (BEK cellulose)	NA	NA	0	NA	1050
2	1.5	2.4 ± 0.2	0.60 ± 0.05	0	25 ± 4	150 ± 10
3	3	2.8 ± 0.1	0.68 ± 0.1	0	23 ± 6	120 ± 10
4	6	3.1 ± 0.2	0.75 ± 0.1	0	19 ± 7	100 ± 20
5	9	2.9 ± 0.2	0.70 ± 0.2	0	20 ± 5	80 ± 5

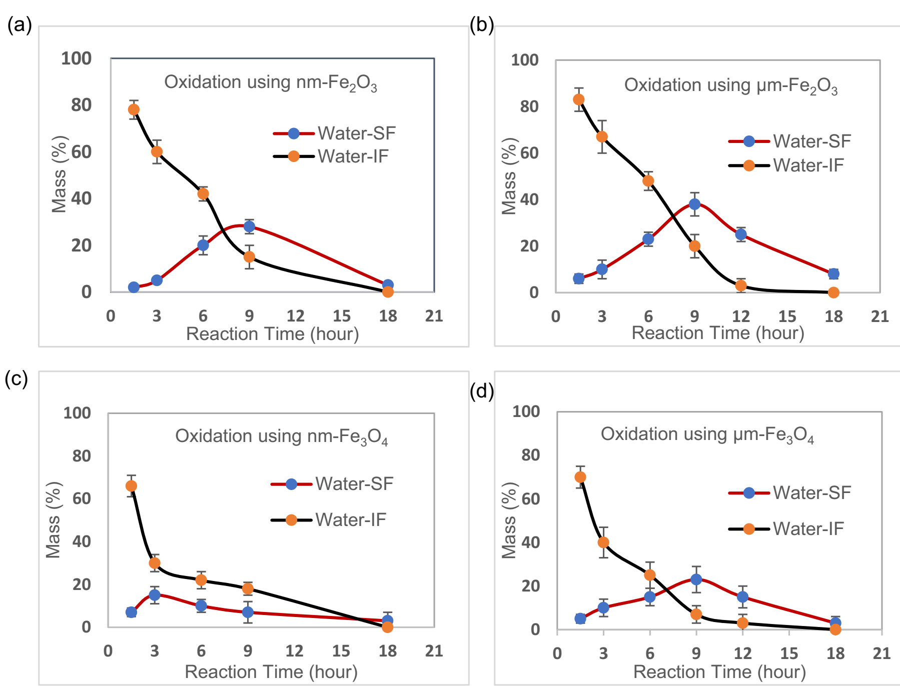

Fig. 2. % yield of Water-IF and Water-SF as a function of reaction time using (a) nm-Fe_2O_3, (b) μm-Fe_2O_3, (c) nm-Fe_3O_4, (d) μm-Fe_3O_4 as catalysts.

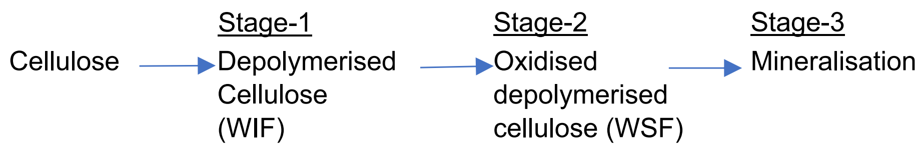

Fig. 3. Flow chart representing different stages involved in cellulose oxidation.

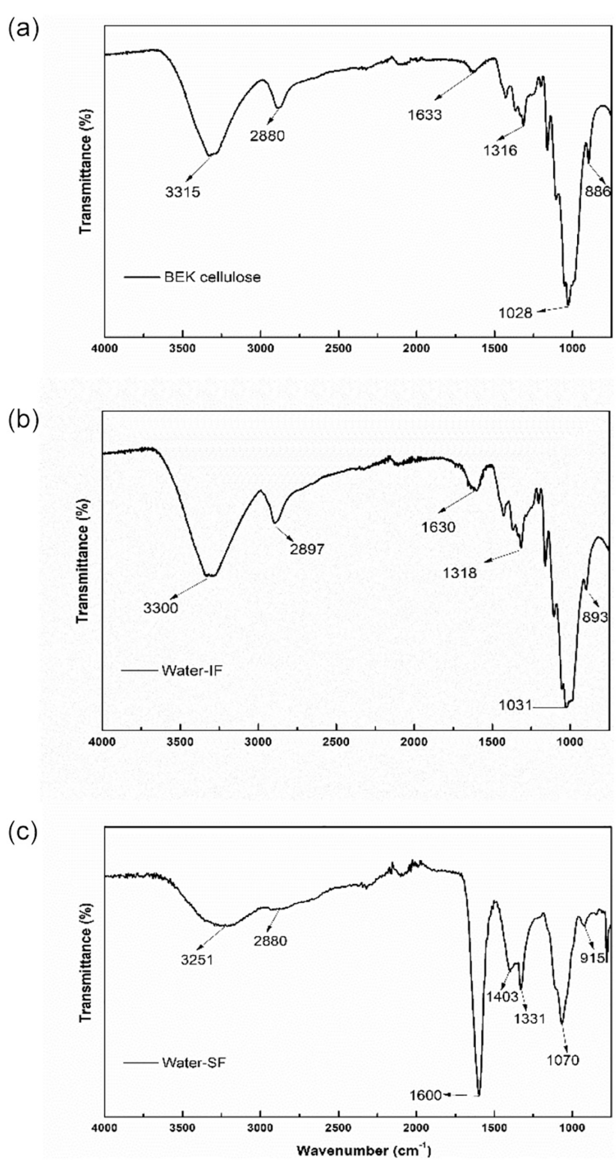

Fig. 4. IR spectra of (a) BEK cellulose, (b) Water-IF (c) Water-SF.

inexpensive filtration methods can be adapted for purification because of their higher specific gravity and insoluble nature in its oxide form (used in this research) (Abdulraheem et al., 2020; Ityel, 2011). Therefore, iron oxides are highly suitable as a catalyst. Further, in nature, iron oxide acts as a potent oxidising agent (Pereira et al., 2012; Sadri et al., 2014). So, we hypothesised that conducting iron oxide-hydrogen peroxide oxidation on cellulose would result in a sustainable method of producing nanocellulose fibres from cellulose.

In this study, two iron oxide catalysts are utilised, hematite (Fe_2O_3) and magnetite (Fe_3O_4). The iron oxides, when treated with hydrogen peroxide, give rise to OH• radicals. This kind of reaction is called a heterogeneous Fenton like process. Reaction kinetics of Fe^{2+} ions with hydrogen peroxide is much higher (63–76 M^{-1} s^{-1}) than Fe^{3+} ions (0.001–0.01 M^{-1} s^{-1}). As a result, the reaction of Fe_3O_4 (with both Fe^{2+} and Fe^{3+} ions in its crystal lattice) is expected to be more rigorous than that of Fe_2O_3 (only Fe^{3+} ions in its crystal lattice) (Pereira et al., 2012). In this research, to avoid the uncontrolled reaction, divalent Fe_2O_3 is predicted to be preferable over Fe_3O_4.

In literature, Fenton like reactions is extensively used for wastewater treatment (Mohajerani et al., 2009) and dye degradation (Nidheesh et al., 2013), where the complete decomposition of organic compounds takes place with the ultimate production of nontoxic H_2O and CO_2 with time. Some researchers have used Fenton reactions on cellulose using iron salts such as iron sulfate as catalysts (Li et al., 2018; Yang et al., 2019). The main drawback of this process is that in iron sulfate, because of the presence of free Fe^{2+} ions, the reaction must be conducted in acidic media to avoid the precipitation of the iron hydroxide at pH > 3. In comparison, iron oxide catalysts work in a broad range of pH.

Thus, the usage of Fe_2O_3 or Fe_3O_4 catalysts has an advantage over iron salt catalysts. Additionally, none of the papers about Fenton reactions on cellulose has discussed the production of water-soluble oxidised cellulose and the stages involved in the process.

This study investigates the oxidation of cellulose with Fe_2O_3 and Fe_3O_4 of two different particle sizes, one being 50 nm, and another is 1 μm. The oxidation yield was measured as the function of reaction time, using each catalyst to identify the best reaction condition. Nanometre sized catalyst is believed to be more effective than the micrometre sized catalyst with its better approachability. The products were analysed to find the carboxyl content, degree of polymerisation, crystallinity, and morphology using FTIR, XPS, NMR, XRD, and SEM analysis. By analysing the results, the possible different stages involved in the reaction were explained.

2. Experimental section

2.1. Materials

Bleached eucalyptus kraft (BEK) cellulose pulp (~12 wt% solid content) was supplied by Australian Paper, Maryvale, Australia, which is having a native cellulose allomorph. This BEK cellulose is a standard grade used for fine paper production. All chemicals are analytical grade and used without further purification. Hydrogen peroxide (H_2O_2) solution (30 wt% in water), Fe_2O_3 50 nm, Fe_2O_3 1 μm, Fe_3O_4 50 nm, Fe_3O_4 1 μm, anhydrous sodium hydroxide (NaOH) were purchased from Sigma Aldrich. The filter paper used for the filtration was Advantec 90 mm, grade no. 2, purchased from Labtek Pty Ltd.

2.2. Production of nanocellulose fibres and water-soluble cellulose derivatives

Below is the typical procedure used for the synthesis. BEK cellulose (8.3 g, 12% solid content, 1.0 g dry weight, 6.1 mmol (considering molecular weight of anhydrous glucose unit)) was taken in a round bottomed flask with 35 ml of deionised water. The mixture was sonicated for 5 min. Next, 10 mol% (based on the anhydroglucose units) of iron oxide (Fe_2O_3 or Fe_3O_4) (50 nm or 1 μm) was added to the flask and sonicated for 10 min. The mixture was heated to 90 °C with stirring 33 ml of 30 wt% H_2O_2 was added to the reaction mixture twice, first at the beginning of the reaction and next at the middle of the reaction (for

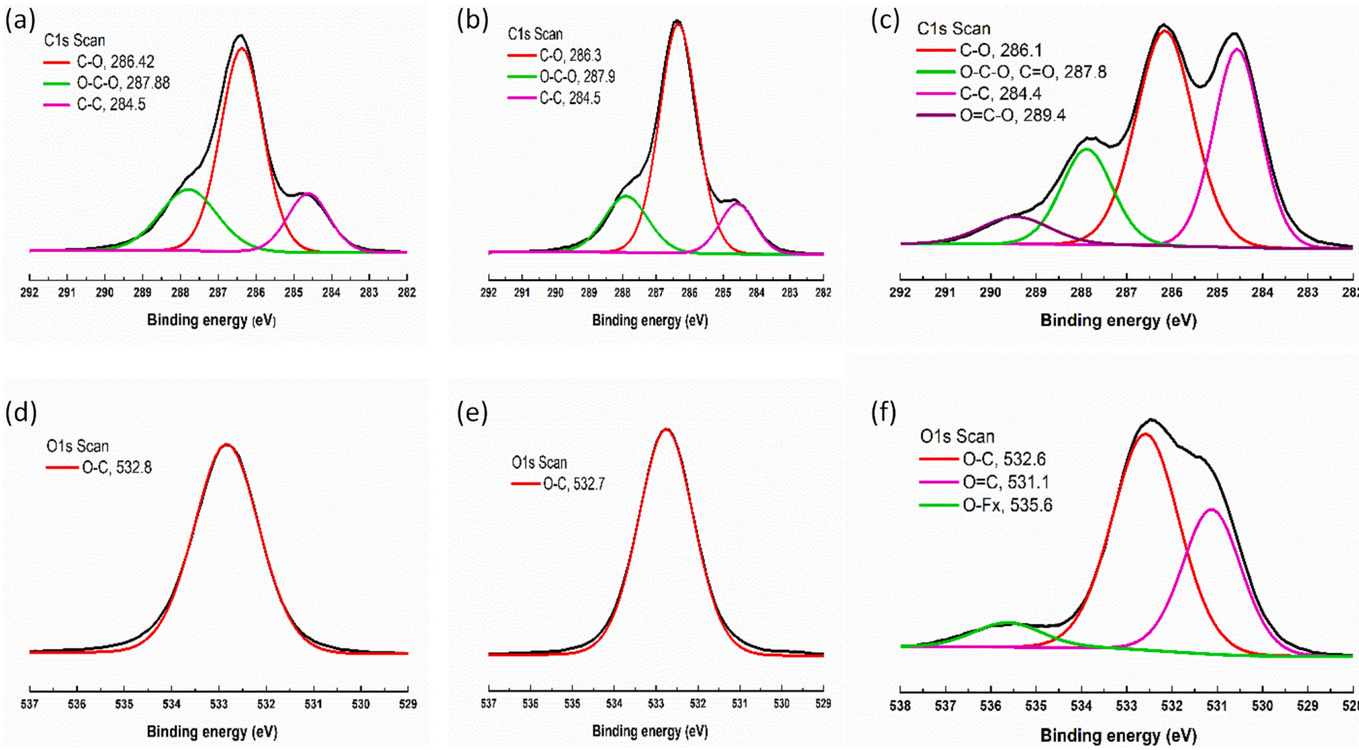

Fig. 5. XPS analysis of BEK cellulose ((a) C1s scan, (d) O1s scan); Water-IF ((b) C1s scan, (e) O1s scan) and Water-SF ((c) C1s scan, (f) O1s scan).

example, after 4.5 h for a total 9 hour reaction). The reaction times investigated ranged from 1.5 to 18 h.

The reaction mixture was cooled to room temperature, and 0.5 N NaOH solution was slowly added until the pH of the mixture reaches pH 8–9. The mixture was stirred for 30 min and filtered. The separated solid was stirred in a beaker with 20 ml DI water for 5 min and filtered and dried in an oven. This water-insoluble fraction (Water-IF) was then characterised as described below.

The filtrate was centrifuged to collect the supernatant by separating it from the remaining catalyst. 70 ml of ethanol was added to the supernatant to precipitate the water soluble product. The product was filtered and dried using a freeze drier to obtain a white solid. This water soluble fraction (Water-SF) was then characterised as described below.

The pictorial representation of the reaction mixture (BEK cellulose with μm-Fe_2O_3 and H_2O_2), Water-SF, and Water-IF are given in Fig. 1. The image of the dispersion of 1% Water-IF in water is given in Supplementary information in Fig. S2.

2.3. Characterisation methods

Agilent Cary 630 FTIR was used for IR spectroscopy measurements. Scanning electron microscopy (SEM) was performed using FEI Nova NanoSEM 450 equipped with a field-emission source at 5 kV. The sample preparation for SEM was done by diluting the sample to 0.005 wt% and 0.0005 wt% in ethanol. 10 μl of the prepared sample was pipetted onto carbon stubs and air-dried. The sample was then coated with iridium with 2 nm thickness.

The average degree of polymerisation (DPv) was determined by measuring the intrinsic viscosity of the sample solutions in cupriethylenediamine (CED) solution. Then the DPv values were determined using Mark-Houwink-Sakurada equation (Eq. (1))

$$[\eta] = 0.57 \times \mathrm{DPv}. \tag{1}$$

where $[\eta]$ is the average intrinsic velocity (Zimmermann et al., 2010).

Carboxyl content of the samples was measured by a conductometric titration analysis using Mettler Toledo T5 titrator (Shinoda et al., 2012). The carboxyl content was calculated by using the equation,

$$\text{Carboxyl content (mmol/g)} = C \times (V_2 - V_1)/w \tag{2}$$

where $(V_2 - V_1)$ is the volume of NaOH solution to neutralise the carboxylic group (ml). C is the sodium hydroxide concentration (mol/l), w is the dry sample weight (g). By using these titration values, the degree of substitution (DS) was calculated by using the equation:

$$DS = 162 \times C \times (V_2 - V_1)/w - 111 \times C \times (V_2 - V_1) \tag{3}$$

where 162 is the molar mass of the anhydrous glucose unit (AGU), 111 is the molar mass difference of fully carboxylated 2,3,6-tricarboxycellulose and AGU (da Silva Perez et al., 2003). Degree of substitution was expressed as the ratio of the amount of sodium carboxylate group per hydroxyl group in AGU.

Homogenisation of the sample with 0.5% solid content was performed for single pass using GEA Niro Soavi Homogeniser Panda at high pressure of 600 bar. Sonication of the sample with 0.5% solid content was carried out for 10 min using Elmasonic S 100 ultrasonic bath with 220–240 V and 37 kHz ultrasonic frequency.

Surface chemical analysis of BEK cellulose, Water-IF, and Water-SF were carried out using Thermo Scientific Nexsa XPS spectrometer equipped with an Al Kα irradiation source. Survey scans were generated from −10 to 1350 eV with a scan step of 1 eV. High-resolution C1s and O1s spectra were recorded from 279 to 298 eV and 526 to 544 eV, respectively. Thermo Avantage software was used to perform data processing and analysis.

Ash content of BEK cellulose and Water-IF was analysed by heating 1 g of oven-dried sample in a crucible using a muffle furnace at 550 °C for 5 h. The inorganics that remained in the crucible were weighed gravimetrically to a constant weight.

X-ray diffraction (XRD) of BEK cellulose and Water-IF were done by using Bruker D8 Advance Eco Diffractometer with 1000 W Co-anode X-ray source with Fe Kβ filters. X-ray diffractograms were recorded at diffraction angle 2θ = 5°–60°. Air dried fibre sheets (samples) were

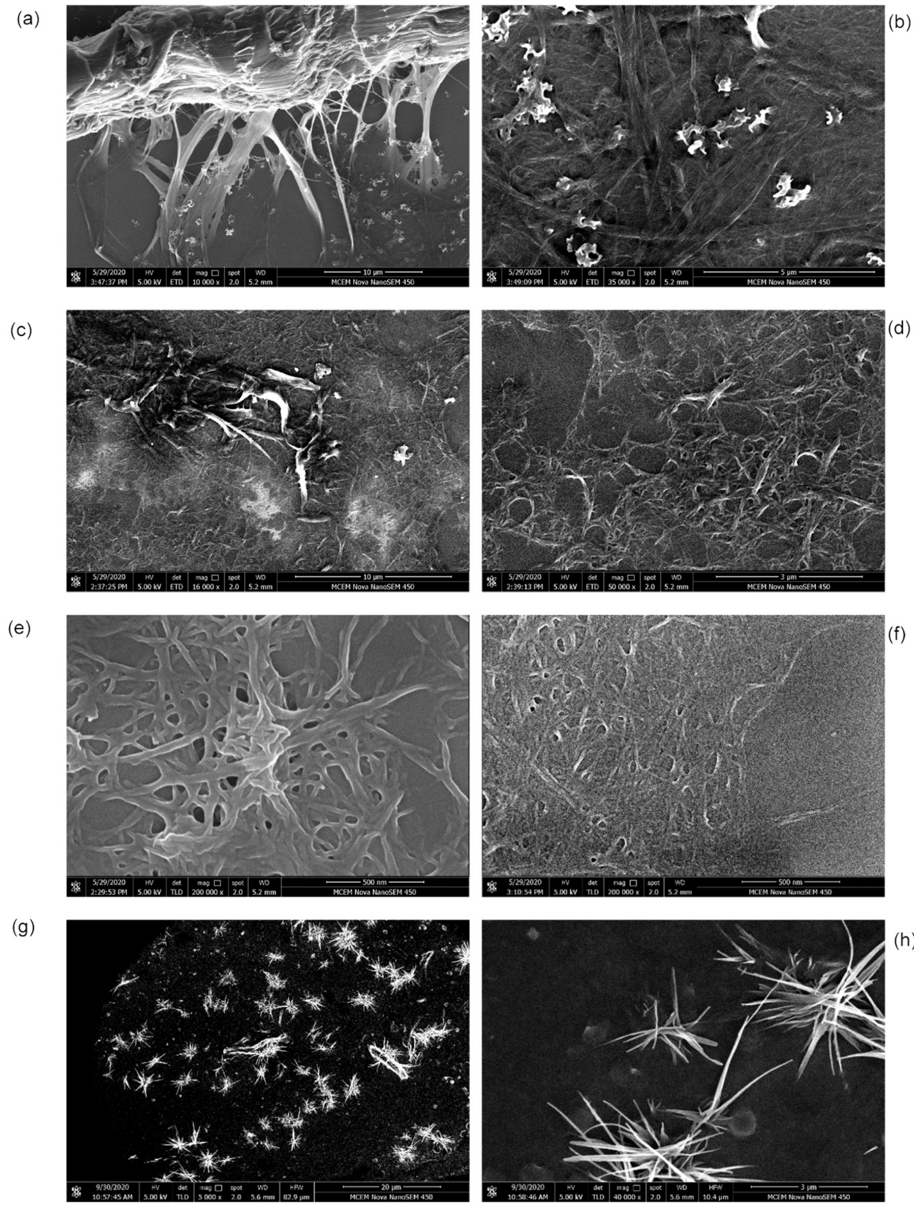

Fig. 6. SEM images of (a), (c) BEK cellulose and homogenised Water-IF of 0.005% concentration at 10,000 x magnification. Images (b), (d) BEK cellulose and homogenised Water-IF of 0.005% concentration at 50,000× magnification. Images (e) and (f) sonicated Water-IF and homogenised Water-IF of 0.005% concentration at 200,000× magnification. Images (g) and (h) sonicated Water-IF of 0.0005% concentration at 5000× and 40,000× magnification respectively.

prepared from 1% slurry of fibre in water. The crystallinity index was calculated from the ratio of the area of the crystalline region to the total area of the curves.

3. Results and discussion

The first part of the paper investigates different catalysts and sizes, while the second part of the paper concentrates on properties obtained at the best reaction conditions.

3.1. Oxidation reaction of cellulose using iron oxide catalysts

The oxidation reactions of cellulose were carried out using four different iron oxide catalysts (10 mol%), namely: 50 nm size Fe_2O_3 (nm-Fe_2O_3), 1 μm size Fe_2O_3 (μm-Fe_2O_3), 50 nm size Fe_3O_4 (nm-Fe_3O_4) and 1 μm size Fe_3O_4 (μm-Fe_3O_4) at different interval of times. The experiments that produced a water-insoluble fraction (Water-IF) and a water-soluble fraction (Water-SF) after the oxidation reaction are summarised in Fig. 2. The average of three experimental values has been taken, and the percentage yield is calculated.

All the catalysts, nm-Fe_2O_3, nm-Fe_3O_4, μm-Fe_2O_3 and μm-Fe_3O_4, gave both Water-SF and Water-IF products. However, the yield of the products was varying with respect to the duration of the reaction, as discussed below:

As it can be seen in Fig. 2(a), the oxidation of cellulose using nm-Fe_2O_3 gave a maximum yield of 78% of Water-IF when the reaction was carried out for 1.5 h (Fig. 2(a) black line). It formed 2% of Water-SF from the same reaction (Fig. 2(a) red line). The remaining 20% was not collected in any form; this result indicated that this part of the cellulose was decomposed to water and carbon dioxide by the strong oxidation of hydroxyl radicals generated. As the reaction duration was continued, the yield of Water-IF decreased gradually, and the yield of Water-SF increased. When the reaction duration was 9 h, 28% of Water-SF, 15% of Water-IF was obtained. When the reaction was carried out beyond 9 h, both Water-IF and Water-SF degraded drastically, and after 18 h (Fig. 2 (a) red line), only a trace amount of Water-SF was obtained.

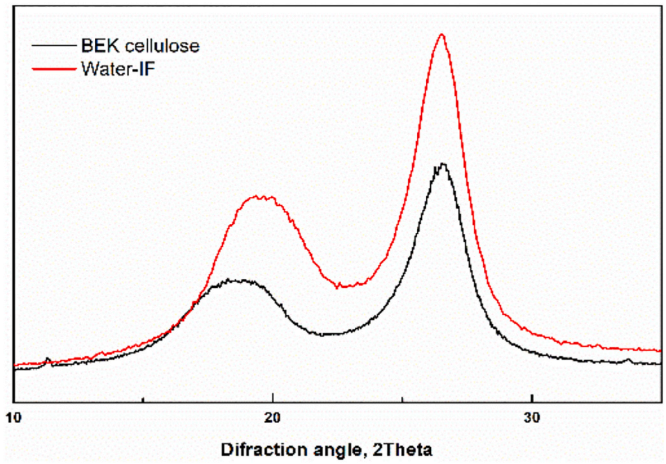

Fig. 7. XRD spectra of BEK cellulose and Water-IF.

When nm-Fe_3O_4 was utilised for the reaction within a 1.5-hour reaction, only 66% of Water-IF (Fig. 2(c), black line) and 7% of Water-SF (Fig. 2(c), red line) was recovered. The remaining 27% was not collected in any form. When the reaction duration was 3 h, a maximum of 15% of Water-SF (Fig. 2(c), red line) was recovered, with 30% of Water-IF (Fig. 2(c), black line). Beyond 3 h of reaction, both Water-SF and Water-IF degraded drastically.

By comparing the results of nm-Fe_2O_3 and nm-Fe_3O_4 (discussed above), the cellulose degradation is faster for the nm-Fe_3O_4 than nm-Fe_2O_3. This faster degradation can be explained as follows: nm-Fe_2O_3 contains only Fe^{3+} ions in its crystal lattice, whereas nm-Fe_3O_4 contains Fe^{2+} and Fe^{3+} ions in its crystal lattice. The rate of generation of hydroxyl radicals from Fe^{2+} ion with hydrogen peroxide is much faster than that of Fe^{3+} ion with hydrogen peroxide (Pereira et al., 2012).

Hence with nm-Fe_3O_4, more and more hydroxyl radicals will be produced at a given time compared to that with nm-Fe_2O_3. Therefore, the reaction will be faster in the case of nm-Fe_3O_4 than nm-Fe_2O_3. As a result, the degradation of cellulose is also faster in the case of nm-Fe_3O_4. Hence to achieve controlled oxidation of cellulose, the nm-Fe_3O_4 catalyst is less favoured.

μm-Fe_2O_3 catalyst (Fig. 2(b) (black line)) gives the maximum yield (out of all the reactions tried in this research) of Water-IF, i.e., 83% after a 1.5-hour reaction. The same catalyst also gave a maximum yield of Water-SF, i.e., 38% after a 9-hour reaction (Fig. 2(b), red line). In the case of reactions using μm-Fe_3O_4 (Fig. 2(d)) degradation was faster as compared to μm-Fe_2O_3 (Fig. 2(b)) (same explanation as explained above about the Fe^{2+} and Fe^{3+} ions hold good here also).

When the yields of Water-IF and Water-SF at a given time using nanometre catalysts (Fig. 2(a) and (c)) and micrometre catalysts (Fig. 2 (b) and (d)) are compared, micrometre catalysts gave better yield than that of nanometre catalyst. This better yield can be explained as follows: The micrometre catalysts being bigger particles, have poor accessibility of cellulose molecules, thereby lower the degradation of cellulose.

As a result, the performance of all the catalysts depends on the particle size of the catalyst and the divalent or trivalent ions present in the crystal lattice of the catalyst. I.e. in order to achieve controlled oxidation of cellulose and obtain the highest yields of products, Fe_2O_3 catalyst is better than Fe_3O_4 catalyst, and a micrometre sized particular catalyst is more suitable than that of a nanometre sized catalyst. Hence the order of the catalyst's performance on cellulose can be represented as μm-Fe_2O_3 ≥ nm-Fe_2O_3 > μm-Fe_3O_4 > nm-Fe_3O_4. μm-Fe_2O_3 is considered the best-suited catalyst for obtaining a maximum yield of Water-IF of 83% and Water-SF of 38% after the time interval of 1.5 and 9 h, respectively.

3.2. Characterisation of Water-SF and Water-IF

μm-Fe_2O_3 being the most suitable catalyst with the highest fraction of reaction products among the others, the Water-IF and Water-SF obtained by cellulose with μm-Fe_2O_3 were analysed in detail to confirm their chemical structure after the oxidation.

3.2.1. Degree of polymerisation, degree of substitution, and carboxyl content and ash content

Carboxyl content of Water-SF and Water-IF obtained by the reaction of cellulose with μm-Fe_2O_3 at different reaction time intervals was analysed. As shown in Table 1, column 3, the carboxyl content of the Water-SF was almost equal to 2.9 mmol/g, irrespective of the reaction time. The carboxyl content of Water-IF (Table 1, column 5) from different reaction times was zero. These results suggest that the Water-IF was not oxidised at any point in time. In comparison, Water-SF is a highly oxidised fraction. The degree of substitution (DS) of the Water-SF (Table 1, column 4) was in the range of 0.60–0.75. DS is the fraction of hydroxyl groups within AGU in cellulose that has been converted to a carboxylate group.

Water-SF and Water-IF obtained by the reaction using μm-Fe_2O_3 were tested for their degree of polymerisation (DP). As shown in Table 1, DP of all Water-SF's was found out to be between 19 and 30, and the DP of Water-IF's were in the range of 80–160. In comparison, the DP of BEK cellulose (starting material) was 1050.

Hence a drastic decrease in the DP was witnessed. Also, the DP of all the Water-SF's and Water-IF's were between 19 and 30 and 80 and 160, respectively, when the reaction was carried out for 1.5 to 9 h (Table 1).

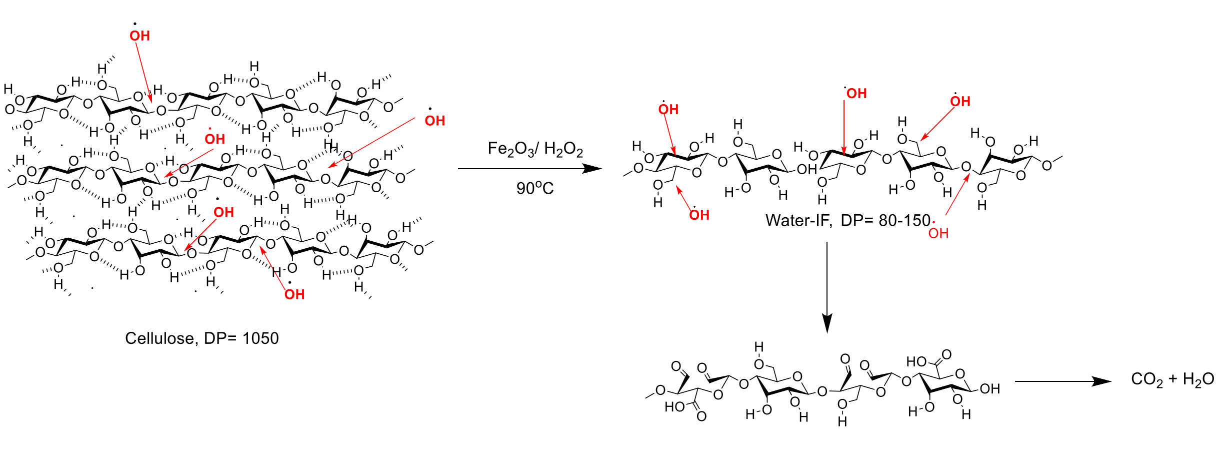

Fig. 8. Proposed reaction scheme representing cellulose oxidation.

The combined study of mass yield, carboxyl content and degree of polymerisation of Water-SF and Water-IF was done to draw the following conclusions. When the reaction was carried out for 1.5 h, 83% of Water-IF was formed (Section 3.1, Fig. 2(b) black line). This Water-IF was having DP, 150 ± 10. So, within 1.5 h of reaction, BEK cellulose with 1050 DP was defibrillated to Water-IF. Also, the carboxylic content of Water-IF was 0. That suggests that the Water-IF was the highly defibrillated, non-oxidised fraction. The carboxylic content test also indicates that the Water-IF's surface chemistry is the same as that of BEK cellulose.

When the reaction was continued for 9 h (Fig. 2(b) red line), the maximum yield of Water-SF (38%) was obtained. This Water-SF was having a DP of around 25, with carboxylic content, around 2.9 mmol/g. This result strongly suggests that Water-SF is an oligomeric, highly oxidised fraction collected from the reaction mixture.

BEK cellulose and Water-IF (obtained from a 1.5-hour reaction of cellulose with μm-Fe_2O_3) were analysed to find the inorganic matters in the sample. Ash content of BEK cellulose was 0.1 ± 0.02%, and that of Water-IF was 0.3 ± 0.1%. This 0.2 ± 0.1% increase in ash content suggests the amount of iron oxide trapped in the Water-IF.

All the above observations indicate that cellulose undergoes a reaction with μm-Fe_2O_3 and hydrogen peroxide in three stages (Fig. 3). First, cellulose undergoes severe depolymerisation without undergoing oxidation. Next, once the DP is reduced to around 100, the hydroxyl group in depolymerised cellulose could be oxidised to achieve a high carboxyl content of 2.9 mmol/g. This high carboxyl content and low DP resulted in the dissolution of the oxidised cellulose in water. Thus, the Water-SF was formed. At last, this formed Water-SF is entirely decomposed to carbon dioxide and water when the reaction time is longer than 18 h.

3.2.2. *IR spectroscopy analysis*

The IR spectra of BEK cellulose (starting material), Water-IF (Fig. 2(b) black line), 1.5-hour reaction, 83% yield, and Water-SF (Fig. 2(b) red line), 9 h reaction, 38% yield using μm-Fe_2O_3 are given in Fig. 4.

IR-spectrum (a) of BEK cellulose shows a prominent broad peak at the region from 3000 to 3700 cm^{-1}, which corresponds to the -OH stretching vibrations of the hydroxyl group. This OH stretching vibration peak has drastically reduced in the case of IR-spectrum (c) of Water-SF. This reduction in OH stretching indicates the transformation of the -OH group in Water-SF. A prominent new peak at 1600 cm^{-1} has appeared in Water-SF, which corresponds to the C=O stretching vibrations of the carbonyl group. Also, a peak at 1400 cm^{-1} has appeared in Water-SF, which corresponds to free -COO- stretching of the sodium carboxylate group.

A peak at 1100–1000 cm^{-1}, which corresponds to the C-O-C stretching vibrations of β (1–4) linkage, is prominent in IR-spectra (a) of BEK cellulose. Whereas in the Water-SF spectrum (c), the peak intensity has reduced drastically. This reduction in C-O-C stretching indicates the severe breakage of the glycosidic bond in Water-SF. A peak at 2900 cm^{-1} which corresponds to C—H stretching vibrations, got reduced in Water-SF spectra (c). These results strongly support the -OH groups' oxidation to carboxyl groups in Water-SF in the spectrum (c). Spectra (b) represent IR spectra of Water-IF separated after a 1.5-hour reaction. The spectrum (b) shows that all the peaks correspond to that of the spectrum (a), thus confirming that the Water-IF has not undergone oxidation.

3.2.3. *XPS analysis*

XPS analysis of BEK cellulose, Water-IF, and Water-SF (1.5 h and 9 h reaction respectively using μm-Fe_2O_3) are given in Fig. 5.

Fig. 5(a) and (b) is the C1s scans of cellulose and Water-IF, respectively. The binding energies of Water-IF exactly match that of cellulose. Similarly, O1s scans of cellulose and Water-IF ((d) and (e)) are also showing the same binding energy pattern, which supports our hypothesis that the Water-IF is a non-oxidised fraction. Whereas (a) and (c) are C1s scans of cellulose and Water-SF, there is a drastic difference in the binding energy pattern. The binding energy of carbon attached to two oxygen atoms (C=O, O-C-O) at 287.8 eV has increased in the case of Water-SF. Additionally, the appearance of a new peak at 289.4 in Water-SF, which corresponds to the carbonyl peak, confirms the formation of the carboxyl group in Water-SF. Also, by comparing (d) and (f), which are the O1s scans of cellulose and Water-SF; in (f), along with O—C bond binding energy (at 532.6), O=C bond binding energy (at 531.1) is also very prominent. These results strongly support the oxidation of cellulose in Water-SF.

3.2.4. *Morphology of Water-IF*

The morphology of Water-IF obtained by a 1.5 h reaction of cellulose with μm-Fe_2O_3 was analysed using scanning electron microscopy (SEM). The sample preparation was carried in two different ways. One sample was subjected to homogenisation. Another sample was subjected to sonication to disperse fibres in water. Both samples and BEK cellulose were viewed under scanning electron microscopy (SEM), as shown in Fig. 6. Images, Fig. 6(a) and (c) are BEK cellulose and *homogenised* Water-IF at 10,000× magnification. By comparing the fibre dimensions of Fig. 6(a) and (c), it is clear that, in image (c), the fibres are broken down to small fibres and well dispersed as compared to image (a). Similarly, Fig. 6 images (b) and (d) are images of BEK cellulose and *homogenised* Water-IF at higher 50,000 x magnification. Image (d) shows a well-dispersed nanostructure of Water-IF.

Images Fig. 6(e) and (f) represented the *sonicated* Water-IF and *homogenised* Water-IF respectively at higher, 200,000× magnification. It can be observed that, in both images, fibres are uniformly distributed nanosized fibres. Finally, images (g) and (h) are the *sonicated* Water-IF at lower concentration (0.0005%) at 5000× and 40,000× magnification respectively. In both Fig. 6(g) and (h), the individual fibres can be seen. Hence, the similarity in fibre distribution of *homogenised* sample and *sonicated* sample indicates that the Water-IF separated from reaction does not need a high-pressure homogenisation to obtain well-dispersed fibre, and sonication for 10 min was enough to obtain nanosized fibres.

The size of the fibres was in the range, 30 nm–110 nm thickness and 1–5 μm in length. In comparison, the average thickness and length of starting material (BEK cellulose) were 10–15 μm and 0.6–0.7 mm, respectively. These results conclude that Water-IF is nanocellulose fibres.

3.2.5. *XRD analysis*

XRD analysis of BEK cellulose and Water-IF (1.5-hour reaction of cellulose with μm-Fe_2O_3) is given in Fig. 7. The crystallinity index of BEK cellulose was 53.7 ± 5%. Whereas, crystallinity index of Water-IF was 73 ± 4%. After treatment, the increase in crystallinity of fibres suggests that the OH radicals generated in the reaction react with the less organised, more reactive amorphous region of BEK cellulose by breaking the bonds in the amorphous area. The finding of this investigation complements those of earlier studies. i.e., 83% yield of Water-IF after 1.5-hour reaction was due to the degradation of the amorphous region in BEK cellulose. Thus, the improvement of crystallinity is observed.

The crystallinity index value of Water-IF was similar to nanocrystals obtained by acid hydrolysis and enzyme hydrolysed cellulose (Hafid et al., 2021; Trache et al., 2017). The acid hydrolysis method is an acid-induced destruction process, during which diffusion of acid molecules into cellulose microfibrils occurs, leading to cellulose nanocrystals with a high 70–80% crystallinity. Various acids such as sulfuric acid, hydrobromic acid, hydrochloric acid, phosphoric acid have been used to conduct acid hydrolysis (Camarero Espinosa et al., 2013). At the end of the process, the mixture undergoes a series of separation and washing, rinsing steps followed by the dialysis against deionised water to remove acid from the product (Mariano et al., 2016). Compared with the acid hydrolysis method, our method eliminates the need for harsh chemicals and the need for a complicated corrosion-resistant reactor. On the other hand, the enzymatic process for producing nanocellulose has its drawback in prolonged processing time, the lower yield of the product

(10–30%), and the high costs of enzymes (Shankaran, 2018). Our method overcomes these drawbacks by the short processing time of 1.5 h, a high yield of 83% by using economic reagents.

3.2.6. Compositional analysis

The NREL (national renewable energy laboratory method) compositional analytical results of BEK cellulose and Water-IF were given in Supplementary data Table S1. BEK cellulose had 83 ± 2% glucose and 9 ± 1% xylose, and around 7 ± 1.5% total lignin. The NREL compositional analysis of Water-IF showed the complete removal of insoluble lignin and a drastic decrease in xylose content to around 2% (as can be seen in Supplementary data, Fig. S1). The cellulose content (glucose content) of Water-IF was increased to around 90%.

The NREL analytical results indicated that the treatment given to the BEK cellulose in this research had reduced the amount of lignin and hemicellulose present in BEK cellulose, thereby increasing the total cellulose content to 90%. This result gives a very interesting scope for future work to apply the same treatment to the lignocellulose and study the outcome.

3.3. The proposed reaction scheme

We propose the reaction scheme in Fig. 8 by investigating the analytical evidence. Hydroxyl radicals generated in the reaction mixture break the cellulose bonds, preferably in the amorphous region (Section 3.2.5, XRD analysis), to produce nanocellulose (Water-IF) of DP, 80–150 range (Section 3.2.1, DP analysis) with high crystallinity of 73 ± 4 (Section 3.2.5, XRD analysis). The nanocellulose formed is a non oxidised cellulose fraction (Sections 3.2.1, carboxylic content test; 3.2.2, IR analysis; 3.2.3, XPS analysis) with the fibre dimension of 30-110 nm thickness, 1–5 μm in length (Section 3.2.4, SEM analysis). On further continuation of the reaction, Water-IF gets oxidised and dissolved in reaction media to produce Water-SF with DP, 20–25 (Section 3.2.1) Water-SF is the highly oxidised cellulose fraction (Section 3.2.2, IR analysis; Section 3.2.3, XPS analysis) with carboxylic content, 2.4–2.9 mmol/g (Section 3.2.1). Finally, on further continuation of reaction time, the dissolved Water-SF completely oxidises to CO_2 and water (Section 3.1). The best result could be obtained by choosing the appropriate catalyst (Section 3.1). By choosing μm-Fe_2O_3, the maximum yield of Water-IF (83%) was obtained by conducting a reaction for 1.5 h. The maximum yield of Water-SF (38%) was obtained by continuing the reaction for 9 h. Beyond 18 h, all the cellulose was degraded entirely to CO_2 and water (Section 3.1).

4. Conclusion

A simple, promising, one-step method was developed to produce highly crystalline nanocellulose fibre (Water-IF) and oligomeric water-soluble carboxylated cellulose derivative (Water-SF). Three stages involved in the process were proposed with analytical evidence. This work presents a promising alternative to methods requiring more hazardous halogenated oxidants, high-energy mechanical pretreatments, and strong corrosive acids to produce nanofibres and water-soluble carboxylated cellulose derivatives. As predicted, Fe_2O_3 is proven to be a better catalyst than Fe_3O_4 to have a good control over the process. Further, the micrometre size of the catalyst was more suitable than the nanometre size (contrary to the hypothesis).

In this research, the authors have mainly focused on the sustainable method of producing nanofibres and water-soluble oxidised cellulose using renewable materials. The application of the products will be studied in the future.

CRediT authorship contribution statement

Poornima Vijay: Conceptualization, Methodology, Investigation, Formal analysis, Writing – original draft, Writing – review & editing. **Warren Batchelor:** Supervision, Conceptualization, Writing – review & editing, Project administration. **Kei Saito:** Supervision, Conceptualization, Writing – review & editing, Project administration, Funding acquisition.

Declaration of competing interest

The authors declare that they have no known competing financial interests or personal relationships that could have appeared to influence the work reported in this paper.

Acknowledgments

The authors gratefully acknowledge the funding of the Australian Research Council (ARC) and Processing Advance Lignocellulosics (PALS) [grant number-IH170100020]. The authors also acknowledge the Monash School of Chemistry, Monash X-ray Platform, and Monash Centre for Electron Microscopy to use facilities. KS acknowledge the support from Yashima Environment Technology Foundation.

Appendix A. Supplementary data

Supplementary data to this article can be found online at https://doi.org/10.1016/j.carbpol.2021.119060.

References

Abdulraheem, F. S., Al-Khafaji, Z. S., Hashim, K. S., Muradov, M., Kot, P., & Shubbar, A. A. (2020). Natural filtration unit for removal of heavy metals from water. July *IOP Confererence Series: Materials Science and Engineering, 888*(1), 012034. IOP Publishing.

Abitbol, T., Rivkin, A., Cao, Y., Nevo, Y., Abraham, E., Ben-Shalom, T., & Shoseyov, O. (2016). Nanocellulose, a tiny fiber with huge applications. *Current Opinion in Biotechnology, 39*, 76–88.

Arami, H., Khadhar, A., Liggitt, D., & Krishnan, K. M. (2015). In vivo delivery, pharmacokinetics, biodistribution and toxicity of iron oxide nanoparticles. *Chemical Society Reviews, 44*(23), 8576–8607.

Camarero Espinosa, S., Kuhnt, T., Foster, E. J., & Weder, C. (2013). Isolation of thermally stable cellulose nanocrystals by phosphoric acid hydrolysis. *Biomacromolecules, 14*(4), 1223–1230.

Colter, A., & Mahler, R. L. (2006). *Iron in drinking water*. Moscow: University of Idaho.

Collinson, S. R., & Thielemans, W. (2010). The catalytic oxidation of biomass to new materials focusing on starch, cellulose and lignin. *Coordination Chemistry Reviews, 254*(15–16), 1854–1870.

Coseri, S. (2017). Cellulose: To depolymerise… or not to? *Biotechnology Advances, 35*(2), 251–266.

da Silva Perez, D., Montanari, S., & Vignon, M. R. (2003). TEMPO-mediated oxidation of cellulose III. *Biomacromolecules, 4*(5), 1417–1425.

Dimitrijevich, S. D., Tatarko, M., Gracy, R. W., Linsky, C. B., & Olsen, C. (1990). Biodegradation of oxidised regenerated cellulose. *Carbohydrate Research, 195*(2), 247–256.

Elschner, T., Bračič, M., Mohan, T., Kargl, R., & Kleinschek, K. S. (2018). Modification of cellulose thin films with lysine moieties: A promising approach to achieve antifouling performance. *Cellulose, 25*(1), 537–547.

Florence, A., & Attwood, D. (2016). *Physicochemical principles of pharmacy*. London: Pharmaceutical Press.

Hafid, H. S., Omar, F. N., Zhu, J., & Wakisaka, M. (2021). Enhanced crystallinity and thermal properties of cellulose from rice husk using acid hydrolysis treatment. *Carbohydrate Polymers, 260*, Article 117789.

Isogai, A., Hänninen, T., Fujisawa, S., & Saito, T. (2018). Catalytic oxidation of cellulose with nitroxyl radicals under aqueous conditions. *Progress in Polymer Science, 86*, 122–148.

Isogai, T., Yanagisawa, M., & Isogai, A. (2009). Degrees of polymerisation (DP) and DP distribution of cellouronic acids prepared from alkali-treated celluloses and ball-milled native celluloses by TEMPO-mediated oxidation. *Cellulose, 16*(1), 117–127.

Ityel, D. (2011). Ground water: Dealing with iron contamination. *Filtration & Separation, 48*(1), 26–28.

Khan, A. S., Man, Z., Bustam, M. A., Kait, C. F., Nasrullah, A., Ullah, Z., & Muhammad, N. (2018). Dicationic ionic liquids as sustainable approach for direct conversion of cellulose to levulinic acid. *Journal of Cleaner Production, 170*, 591–600.

Li, O. L., Ikura, R., & Ishizaki, T. (2017). Hydrolysis of cellulose to glucose over carbon catalysts sulfonated via a plasma process in dilute acids. *Green Chemistry, 19*(20), 4774–4777.

Li, Q., Wang, A., Long, K., He, Z., & Cha, R. (2018). Modified Fenton oxidation of cellulose fibers for cellulose nanofibrils preparation. *ACS Sustainable Chemistry & Engineering, 7*(1), 1129–1136.

Li, Z., Yang, X., Li, W., & Liu, H. (2019). Stimuli-responsive cellulose paper materials. *Carbohydrate Polymers, 210*, 350–363.

Liu, Y., Chen, W., Xia, Q., Guo, B., Wang, Q., Liu, S., & Yu, H. (2017). Efficient cleavage of lignin-carbohydrate complexes and ultrafast extraction of lignin oligomers from wood biomass by microwave-assisted treatment with deep eutectic solvent. *ChemSusChem, 10*(8), 1692–1700.
Mariano, M., Cercená, R., & Soldi, V. (2016). Thermal characterisation of cellulose nanocrystals isolated from sisal fibers using acid hydrolysis. *Industrial Crops and Products, 94*, 454–462.
Mohajerani, M., Mehrvar, M., & Ein-Mozaffari, F. (2009). An overview of the integration of advanced oxidation technologies and other processes for water and wastewater treatment. *International Journal of Engineering and Technology, 3*(2), 120–146.
Nidheesh, P. V., Gandhimathi, R., & Ramesh, S. T. (2013). Degradation of dyes from aqueous solution by Fenton processes: A review. *Environmental Science and Pollution Research, 20*(4), 2099–2132.
Pazzi, J., & Subramaniam, A. B. (2020). Nanoscale curvature promotes hihg yield spontaneous formation of cell-mimetic Giant vesicles on nanocellulose paper. *ACS Applied Materials & Interfaces, 12*(50), 56549–56561.
Pereira, M., Oliveira, L., & Murad, E. (2012). Iron oxide catalysts: Fenton and fentonlike reactions–a review. *Clay Minerals, 47*(3), 285–302.
Sadri, F., Ramazani, A., Massoudi, A., Khoobi, M., Tarasi, R., Shafiee, A., & Joo, S. W. (2014). Green oxidation of alcohols by using hydrogen peroxide in water in the presence of magnetic Fe3O4 nanoparticles as recoverable catalyst. *Green Chemistry Letters and Reviews, 7*(3), 257–264.
Shankaran, D. R. (2018). Cellulose nanocrystals for health care applications. In *Applications of nanomaterials* (pp. 415–459). Elsevier.
Shinoda, R., Saito, T., Okita, Y., & Isogai, A. (2012). Relationship between length and degree of polymerisation of tempo-oxidised cellulose nanofibrils. *Biomacromolecules, 13*(3), 842–849.
Singh, N., Jenkins, G. J., Asadi, R., & Doak, S. H. (2010). Potential toxicity of superparamagnetic iron oxide nanoparticles (SPION). *Nano Reviews, 1*(1), 5358.
Trache, D., Hussin, M. H., Haafiz, M. M., & Thakur, V. K. (2017). Recent progress in cellulose nanocrystals: Sources and production. *Nanoscale, 9*(5), 1763–1786.
Wohlhauser, S., Delepierre, G., Labet, M., Morandi, G. P., Thielemans, W., Weder, C., & Zoppe, J. O. (2018). Grafting polymers from cellulose nanocrystals: Synthesis, properties, and applications. *Macromolecules, 51*(16), 6157–6189.
Yang, J., Tu, M., Xia, C., Keller, B., Huang, Y., & Sun, F. F. (2019). Effect of Fenton pretreatment on C1 and C6 oxidation of cellulose and its enzymatic hydrolyzability. *ACS Sustainable Chemistry & Engineering, 7*(7), 7071–7079.
Zimmermann, T., Bordeanu, N., & Strub, E. (2010). Properties of nanofibrillated cellulose from different raw materials and its reinforcement potential. *Carbohydrate Polymers, 79*(4), 1086–1093.